

UCLA

UCLA Previously Published Works

Title

A Novel Quantitative Computed Tomographic Analysis Suggests How Sirolimus Stabilizes Progressive Air Trapping in Lymphangioleiomyomatosis

Permalink

<https://escholarship.org/uc/item/2jd8n1sv>

Journal

Annals of the American Thoracic Society, 13(3)

ISSN

2325-6621

Authors

Argula, Rahul G
Kokosi, Maria
Lo, Pechin
[et al.](#)

Publication Date

2016-03-01

DOI

10.1513/annalsats.201509-631oc

Peer reviewed

A Novel Quantitative Computed Tomographic Analysis Suggests How Sirolimus Stabilizes Progressive Air Trapping in Lymphangioliomyomatosis

Rahul G. Argula¹, Maria Kokosi², Pechin Lo³, Hyun J. Kim³, James G. Ravenel⁴, Cristopher Meyer⁵, Jonathan Goldin³, Hye-Seung Lee⁶, Charlie Strange^{1*}, and Francis X. McCormack^{7*}; for the MILES Study Investigators

¹Division of Pulmonary, Critical Care, Allergy and Sleep Medicine and ⁴Department of Radiology, Medical University of South Carolina, Charleston, South Carolina; ²Interstitial Lung Disease Unit, Royal Brompton Hospital, London, United Kingdom; ³Department of Radiology, University of California, Los Angeles, Los Angeles, California; ⁵Department of Radiology, University of Wisconsin, Madison, Wisconsin; ⁶Pediatric Epidemiology Center, University of South Florida, Tampa, Florida; and ⁷Division of Pulmonary, Critical Care, Allergy and Sleep Medicine, University of Cincinnati, Cincinnati, Ohio

ORCID ID: 0000-0002-6184-4093 (R.G.A.).

Abstract

Rationale: The Multicenter International Lymphangioliomyomatosis Efficacy and Safety of Sirolimus (MILES) trial demonstrated that sirolimus stabilized lung function and improved measures of functional performance and quality of life in patients with lymphangioliomyomatosis. The physiologic mechanisms of these beneficial actions of sirolimus are incompletely understood.

Objectives: To prospectively determine the longitudinal computed tomographic lung imaging correlates of lung function change in MILES patients treated with placebo or sirolimus.

Methods: We determined the baseline to 12-month change in computed tomographic image-derived lung volumes and the volume of the lung occupied by cysts in the 31 MILES participants (17 in sirolimus group, 14 in placebo group) with baseline and 12-month scans.

Measurements and Main Results: There was a trend toward an increase in median expiratory cyst volume percentage in the placebo

group and a reduction in the sirolimus group (+2.68% vs. +0.97%, respectively; $P = 0.10$). The computed tomographic image-derived residual volume and the ratio of residual volume to total lung capacity increased more in the placebo group than in the sirolimus group (+214.4 ml vs. +2.9 ml [$P = 0.054$] and +0.05 ml vs. -0.01 ml [$P = 0.0498$], respectively). A Markov transition chain analysis of respiratory cycle cyst volume changes revealed greater dynamic variation in the sirolimus group than in the placebo group at the 12-month time point.

Conclusions: Collectively, these data suggest that sirolimus attenuates progressive gas trapping in lymphangioliomyomatosis, consistent with a beneficial effect of the drug on airflow obstruction. We speculate that a reduction in lymphangioliomyomatosis cell burden around small airways and cyst walls alleviates progressive airflow limitation and facilitates cyst emptying.

Keywords: airflow obstruction; computed tomography biomarkers; cyst characteristics; lymphangioliomyomatosis; sirolimus

(Received in original form September 23, 2015; accepted in final form December 4, 2015)

*Co-senior authors.

Supported by the National Institutes of Health Office of Rare Diseases under National Center for Research Resources grants RR01948 (F.X.M., Bruce Trapnell) and RR019259 (Jeffrey P. Krischer, H.-S.L.).

Author Contributions: R.G.A. and C.S.: take responsibility for the content of the article, including the data and the analysis; R.G.A. and C.S.: conception and design; C.S., P.L., J.G., H.-S.L., F.X.M., and M.K.: data acquisition and synthesis; R.G.A., C.S., F.X.M., H.-S.L., and H.J.K.: analysis and interpretation; and R.G.A., C.S., F.X.M., C.M., J.G.R., M.K., J.G., P.L., H.J.K., and H.-S.L.: drafting and editing of the manuscript for important intellectual content.

Correspondence and requests for reprints should be addressed to Rahul G. Argula, M.B.B.S., M.P.H., Division of Pulmonary, Critical Care, Allergy and Sleep Medicine, Medical University of South Carolina, 96 Jonathan Lucas Street, Suite 812 CSB, MSC 630, Charleston, SC 29425. E-mail: argula@muscc.edu

This article has an online supplement, which is accessible from this issue's table of contents at www.atsjournals.org

Ann Am Thorac Soc Vol 13, No 3, pp 342–349, Mar 2016

Copyright © 2016 by the American Thoracic Society

DOI: 10.1513/AnnalsATS.201509-631OC

Internet address: www.atsjournals.org

Lymphangiomyomatosis (LAM) is a rare, progressive lung disease that primarily affects women and is associated with mutations in tuberous sclerosis genes. The disease course is marked by the development of numerous cysts in the lung parenchyma and progressive airflow obstruction (1). Destructive lung remodeling in LAM is thought to be driven by proliferating smooth muscle cells (LAM cells) that arise from an unknown source, circulate through the blood and lymphatics, infiltrate the lung interstitium, and secrete matrix-degrading enzymes (2).

Understanding of the pathogenesis of LAM has been greatly accelerated by the discovery of tuberous sclerosis complex (TSC) gene mutations and function. Hamartin and tuberin, the products of the *TSC1* and *TSC2* genes, form a complex that negatively regulates the kinase activity of mammalian target of rapamycin (mTOR), a key signaling node that integrates input from upstream growth factor, energy, and substrate signals and controls cellular growth and movement. Inactivation mutation of TSC alleles derepresses mTOR, leading to unrestricted protein translation and cellular proliferation, as well as expression of lymphangiogenic growth factors such as vascular endothelial growth factor C (VEGF-C) and VEGF-D (3). Elucidation of the importance of mTOR signaling in LAM and TSC has rapidly been translated into effective therapies through clinical trials of mTOR inhibitors in these diseases.

The Multicenter International Lymphangiomyomatosis Efficacy and Safety of Sirolimus (MILES) trial was a double-blind, randomized clinical trial sponsored by the U.S. Food and Drug Administration and the Office of Rare Diseases/National Center for Research Resources. It was designed to study the impact of the mTOR inhibitor sirolimus on lung function of patients with LAM. The results of that study showed that patients taking sirolimus had clinically meaningful stabilization of lung function decline and improvements in quality of life and functional performance compared with the placebo group (4). Patients taking sirolimus also had significant reductions in serum VEGF-D compared with the placebo group (5). The physiologic mechanisms underlying the beneficial effects of sirolimus on lung function are unclear.

Remodeling in both the airway and parenchymal compartments of the lung is thought to contribute to the pathogenesis of airflow obstruction in LAM. The airway contribution to obstruction in LAM is likely due to LAM cell infiltration around the small airways (6), which can also be associated with bronchial hyperresponsiveness (7) and dynamic hyperinflation (8).

One proposed mechanism for cyst formation in LAM is air trapping due to a one-way check valve effect in the distal airways that leads to alveolar expansion. Alternatively, direct tissue damage and remodeling may result from secretion of proteases and other matrix-degrading enzymes from LAM cells. Matrix metalloproteinases and cathepsin K have both been identified in LAM lesions by immunohistochemistry (9). Cystic destruction of the interstitium results in reduction in elastic recoil and a loss of the tethering effect on small airways, exacerbating dynamic collapse and worsening airflow obstruction and promoting a cycle of cyst enlargement. Whether treatments such as sirolimus can favorably affect the number and volume of cysts in patients with LAM remains unknown.

Computed tomography (CT)-based analyses of cyst characteristics with density mask techniques demonstrate good correlations with pulmonary function tests (PFTs) in patients with LAM (10), but they have limited ability to discriminate between closely spaced cysts. These techniques use

density thresholds to identify regions with closely juxtaposed differences in relative attenuation to calculate cyst volumes. Insufficient tissue density differences between cysts can compromise the ability to identify adjacent cysts as separate (Figure 1). In this study, we compared changes in quantitative CT findings in MILES subjects over 12 months on sirolimus or placebo. We employed a novel method of cyst analysis based on a “watershed algorithm” to improve resolution of adjacent cysts. This experimental technique (Figure 2), along with a preliminary study demonstrating robust correlations between cyst characteristics and PFTs, is described elsewhere (11).

Methods

In the MILES study, patients who met enrollment criteria were randomized to receive sirolimus or placebo for 12 months (i.e., the treatment period) and then observed while off therapy through Month 24 (i.e., the observation period) (4). Inspiratory and expiratory high-resolution CT scans were performed at 0, 12, and 24 months among participants at sites that opted to participate in this analysis.

For the purposes of this study, only the baseline and 12-month scans were evaluated. The analysis of CT cyst volume percentage was a prespecified secondary

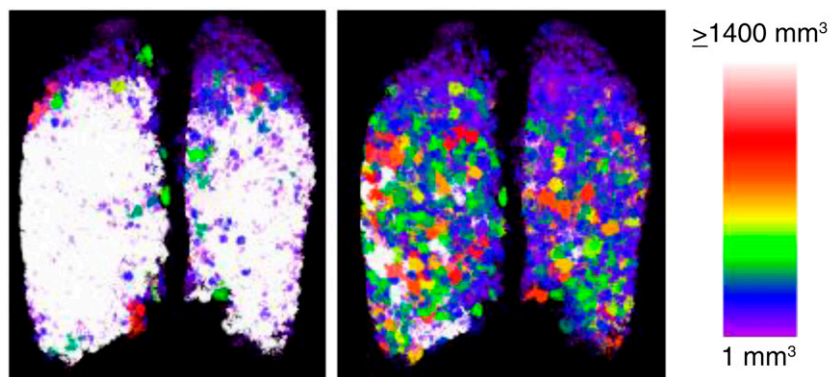


Figure 1. Three-dimensional volume rendering of lymphangiomyomatosis cysts by (left) conventional method which assumes that individual cysts are continuous low-attenuation voxels and (right) the watershed-based method that estimates cyst size by measuring the distance between tissue density peaks. Individual cyst delineation is better using the watershed method than the voxel-based method. The cysts are color coded on the basis of their size, as indicated by the color bar at far right.

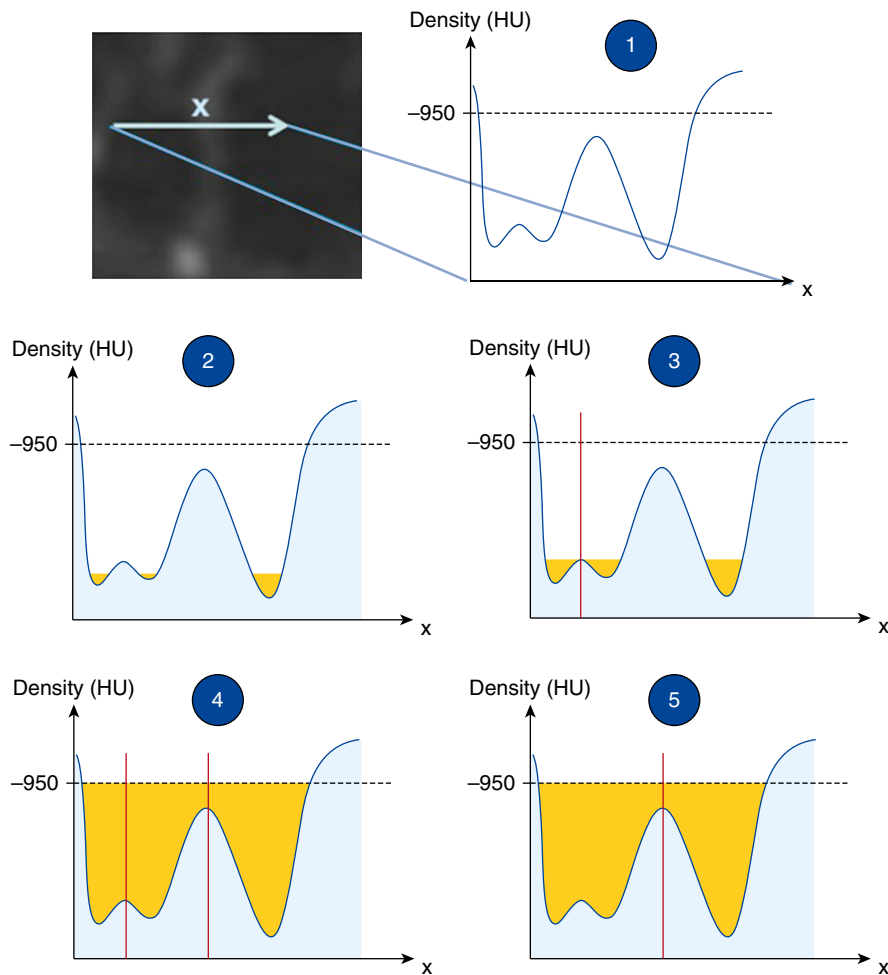


Figure 2. (1) An illustration of the watershed algorithm. (2) Density variations derived from a computed tomographic scan slice are represented on a graph in the form of a terrain with peaks and valleys. (3) Water is filled gradually from the bottom of the valleys. (4) A cyst boundary/wall (red vertical line) is defined as the point where waters from two neighboring valleys meet. (5) The flooding process is finished once all regions below -950 Hounsfield units (HU) are flooded. Regions with weak separation are merged, and cysts are counted (two cysts in this example).

endpoint in the MILES trial. All sites were provided with a CT imaging algorithm and were trained remotely. For the present analysis, we excluded scans of subjects with loculated pneumothorax, areas of consolidation, small pleural effusions, and incomplete imaging of the thorax (Figure 3). To evaluate the possible introduction of bias, the demographic variables and lung function parameters for retained and excluded subjects were compared. Table 1 shows the baseline characteristics of the entire MILES study population and the participants included for the MILES CT analysis.

High-resolution CT images were acquired both at total lung capacity (TLC)

and at residual volume (RV) at 120 kilovolts peak, 160 mA, and 0.6- to 1.25-mm slice thickness using CT scanners from a variety of manufacturers. The postacquisition image processing was performed at the Center for Computer Vision and Imaging Biomarkers, David Geffen School of Medicine, University of California, Los Angeles. The imaging core and analysis team was blinded to the treatment allocation.

Cyst numbers and dimensions were calculated by employing a novel watershed technique to differentiate adjacent cysts using an edge enhancement algorithm to identify subtle edges of each cystic region (11). By analogy to the behavior of rain runoff on either side of a peak, the

watershed is a point in the image that has the greatest voxel density and beyond which the density progressively decreases while moving farther from the point, irrespective of the direction of movement. The algorithm estimates the diameter of a given cyst by measuring the distance between two such watershed points (Figure 2). A threshold voxel index less than -950 Hounsfield units was used in the analysis and indexed to CT-derived volumes at full inspiration (TLC) and expiration (RV), respectively.

Because the cystic spaces in LAM are thought to communicate with the conducting airways, and because both FEV₁ and FVC improved in patients taking sirolimus in the MILES cohort (4), we formulated a prespecified statistical plan to compare the baseline to 12-month changes in expiratory cyst volume percentage (total volume occupied by cysts at RV divided by the RV) between sirolimus- and placebo-treated patients as the primary endpoint. Other secondary variables assessed over the treatment period were change in the inspiratory cyst volume percentage (total volume occupied by cysts at TLC divided by TLC); change in the total cyst number; and changes in CT-derived TLC, RV, VC and RV/TLC. Last, categorical change in cyst size (i.e., small, medium, large) from baseline to 12 months was also compared between the sirolimus and placebo groups.

Statistical Analysis

We compared the between-group differences in mean change from baseline to 12 months for multiple cyst parameters using Wilcoxon rank-sum tests. We also performed an exploratory Markov chain transition matrix analysis to look for differences in dynamic respiratory variation in cyst size gradation from baseline to 12 months between the placebo and sirolimus arms.

The Markov chain transition matrix analysis involved creation of a cyst size transition matrix (from TLC to RV) for each group at baseline and at 12 months. We used three different cyst size thresholds to categorize the cysts into large, medium, and small groups. We then compared cyst size transitions (e.g., large to medium, medium to small) from TLC to RV at baseline with transitions at 12 months for

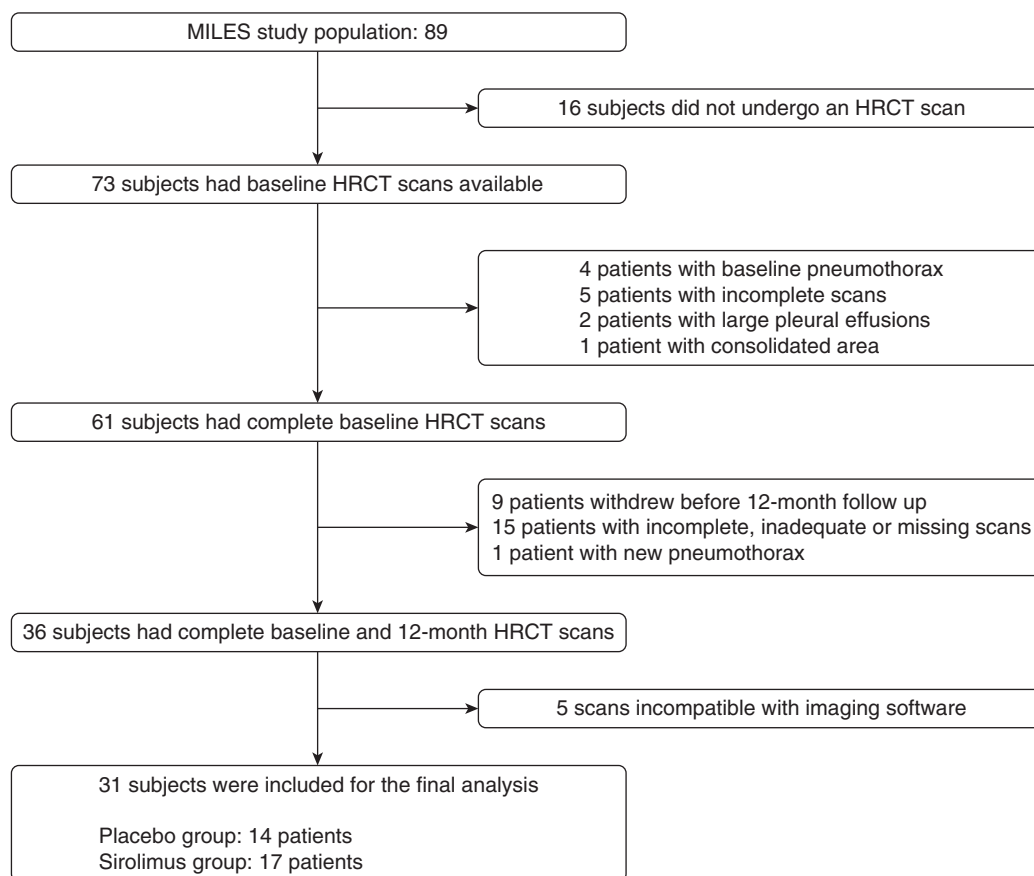


Figure 3. Consolidated Standards of Reporting Trials (CONSORT) diagram showing patient selection for the Multicenter International Lymphangioleiomyomatosis Efficacy and Safety of Sirolimus (MILES) computed tomography cohort. HRCT = high-resolution computed tomography.

both the sirolimus and placebo groups (Table 2).

The laboratory-derived PFT data (included in the online supplement) were also compared between the placebo and sirolimus groups. All statistical operations were conducted using SAS version 9.3 software (SAS Institute, Cary, NC), and two-sided *P* values less than 0.05 were considered statistically significant.

Results

Of a total of 89 patients enrolled in the MILES trial, 16 did not have baseline scans; 5 had inadequate or incomplete scans; and 7 had pleural effusions, consolidations, or acute or chronic pneumothorax. Among the 61 subjects who had usable baseline scans, 9 withdrew before the 12-month time point; 20 had incomplete, inadequate, software-

incompatible, or missing 12-month scans; and one developed pneumothorax. The 31 patients (14 placebo, 17 sirolimus) who had paired sets of baseline and 12-month CT scans that were adequate and available for analysis (Figure 3) composed the MILES CT cohort.

The baseline characteristics of the placebo and sirolimus groups in the MILES CT cohort were not different from those of the MILES cohort as a whole with regard to demographic variables or spirometry (Table 1). There were also no systematic differences in demographic or lung function variables between the patients included in and those excluded from this analysis (see Table E1 in the online supplement). Table 3 shows the between-group comparisons of the baseline to 12-month changes in cyst characteristics. As a point of reference, laboratory-derived PFT data of the MILES CT cohort (spirometry, lung volumes, and diffusing capacity of

carbon monoxide) are included in the online supplement.

Baseline CT-derived variables (e.g., VC, TLC, RV) were similar between the sirolimus and placebo groups. Changes in the various CT-derived variables over the treatment period had no meaningful correlations with changes in FVC, FEV₁, or serum VEGF-D levels (Tables E2–E4). The number of cysts at TLC decreased in both the sirolimus and placebo groups from baseline to 12 months, whereas the number of cysts counted at RV increased in both the groups. These changes were not statistically significant (Table 2). The baseline to 12-month expiratory cyst volume percentage increased in both groups, and the difference was not statistically significant (+2.68% vs. +0.97%, respectively; *P* = 0.10). Inspiratory cyst volume percentage trended higher in both groups but also was not different by treatment allocation (placebo +0.44% vs. sirolimus +1.97%; *P* = 0.60).

Table 1. Baseline characteristics of the Multicenter International Lymphangiomyomatosis Efficacy and Safety of Sirolimus computed tomography cohort

Variable	Placebo (n = 14)	Sirolimus (n = 17)	P Value	
Age, yr	43 (35–55)	44 (42–57)	0.31	
Race			1.00	
	White, n	8	10	
	Asian, n	6	7	
FEV ₁	Volume, L	1.44 (0.96–1.68)	1.18 (1.05–1.46)	0.32
	Percentage of predicted value	52 (35–60)	44 (42–50)	0.62
FVC	Volume, L	3.19 (2.20–3.54)	2.53 (2.03–2.85)	0.15
	Percentage of predicted value	84 (77–99)	75 (66–82)	0.15
FEV ₁ /FVC		0.44 (0.38–0.58)	0.48 (0.41–0.54)	0.65
TLC	Volume, L	5.68 (4.75–6.48)	5.15 (4.59–5.57)	0.13
	Percentage of predicted value	114 (104–130)	102 (97–131)	0.19
FRC, n = 30	Volume, L	3.33 (2.43–3.60)	2.98 (2.27–3.17)	0.22
	Percentage of predicted value	117 (112–129)	109 (101–117)	0.18
RV	Volume, L	2.45 (1.84–2.86)	2.36 (2.13–2.79)	0.86
	Percentage of predicted value	149 (113–209)	149 (113–188)	0.92
DL _{CO} , n = 30	ml/min/mm Hg	12.0 (6.96–14.0)	8.93 (8.30–11.95)	0.65
	Percentage of predicted value	46.7 (33.0–62.6)	43.2 (37.6–49.5)	0.65
Expiratory cyst volume, %		13.89	16.35	0.45

Definition of abbreviations: DL_{CO} = diffusing capacity of carbon monoxide; RV = residual volume; TLC = total lung capacity.

The median values for the age and pulmonary function test variable values are presented. The lower and upper quartiles are represented in parentheses.

Changes in CT-derived lung volumes are presented in Table 4. Baseline to 12-month RV increased in the placebo group to a greater extent than in the sirolimus group (+214.4 ml vs. +2.92 ml, respectively; $P = 0.05$), while TLC increased only slightly in both groups (+19 ml vs. +25.5 ml, respectively; $P = 0.77$), resulting in a between-group divergence in the RV/TLC ratio (+0.05% vs. -0.01%; $P < 0.05$). Consistent with these changes,

vital capacity declined in the placebo group and trended higher in the sirolimus group (-190 ml vs. +15.4 ml, respectively; $P = 0.06$).

To explore the mechanism of improvement in airflow and reduction in air trapping, we performed a Markov chain analysis in which we compared the respiratory cycle variation in cyst size (from TLC to RV) between two time points (baseline and 12 mo) for the placebo and sirolimus groups. The

results show that, at baseline, a significant number of cysts became smaller at full expiration (RV) in both the groups; that is, large cysts became medium or small sized and medium cysts became small sized as lung volume decreased from TLC to RV. At 12 months, the respiratory cycle transition in cyst volumes from large or medium to small during expiration was attenuated in the placebo group, whereas it was preserved in the sirolimus group (Table 2).

Table 2. The Markov-chain cyst-transition (from TLC to RV) matrix analysis

Cyst Volume Definitions	Cyst Size Transition (from TLC to RV)	Number of Cysts Transitioning in Size during Expiration (from TLC to RV)				P Values for Placebo vs. Sirolimus
		Placebo (n = 14)		Sirolimus (n = 17)		
		Baseline, % (SD)	12 Mo, % (SD)	Baseline, % (SD)	12 Mo, % (SD)	
Threshold 1 (small, <50 ml; medium, <200 ml and >50 ml; large, >200 ml)	Medium to small	32 (19)	24 (17)	18 (22)	18 (20)	0.02
	Large to medium	0 (0)	0 (0)	0 (2)	0 (1)	ns
	Large to small	54 (27)	46 (27)	30 (31)	34 (29)	0.02
Threshold 2 (small, <20 ml; medium, <100 ml and >20 ml; large, >100 ml)	Medium to small	13 (14)	8 (10)	7 (10)	5 (8)	ns
	Large to medium	1 (3)	2 (4)	0 (1)	1 (2)	ns
	Large to small	46 (24)	37 (22)	25 (28)	27 (25)	0.005
Threshold 3 (small, <20 mm ³ ; medium, <50 ml and >20 ml; large, >50 ml)	Medium to small	7 (11)	4 (6)	3 (6)	2 (5)	ns
	Large to medium	2 (3)	3 (4)	2 (3)	3 (3)	ns
	Large to small	36 (20)	28 (18)	20 (23)	20 (21)	0.006

Definition of abbreviations: ns = not significant; RV = residual volume; SD = standard deviation; TLC = total lung capacity.

Data are presented as the percentage of LAM cysts transitioning in volume from TLC to RV at baseline and 12 months. Volume categories were arbitrarily defined on the basis of thresholds listed in the left column. The differences from baseline to 12 months in the numbers of cysts transitioning between volume categories during expiration were then compared between the placebo and sirolimus groups.

Table 3. Changes in cyst characteristics from baseline to 12 months

Variable	Placebo (n = 14)	Sirolimus (n = 17)	P Value
Inspiratory			
Change in median inspiratory cyst volume percentage	+0.44% (+0.01%, +2.45%)	+1.97% (−0.12%, +2.96%)	0.60
Change in total cyst number	−495 (−853, −180)	−180 (−1,118, +412)	0.46
Change in median cyst volume, ml	+2.88 (+0.46, +5.02)	+1.72 (+0.52, +5.98)	0.74
Expiratory			
Change in median expiratory cyst volume percentage	+2.68% (+0.62, +4.18)	+0.97% (−0.28, +2.32)	0.10
Change in total cyst number	+676 (−229, +1,704)	+356 (−257, +813)	0.42
Change in median cyst volume, ml	+1.79 (+0.53, +3.36)	+0.42 (−0.32, +3.04)	0.15

Upper and lower quartiles are given in parentheses.

Discussion

The MILES CT cohort analyzed in this study demonstrated, on the basis of spirometric measures, FEV₁ and FVC stabilization while taking sirolimus (Table E5), consistent with the results in the entire MILES cohort (4). In the MILES study, the effect of sirolimus on FVC was disproportionately greater than that for FEV₁, as reported in a prior, smaller trial (12), suggesting a more complex physiologic response than simple relief of airflow obstruction. Quantitative CT analysis was incorporated into the MILES study design to examine the mechanisms of sirolimus effects on pulmonary mechanics and airflow, and to determine if CT parameters could be used as biomarkers to facilitate future clinical trials.

The characteristic changes noted in PFTs in patients with LAM are airflow obstruction, hyperinflation, and air trapping, accompanied by a decrease in diffusing capacity, similar to those of patients with chronic obstructive lung disease (1). LAM cell parenchymal infiltration and pleural processes can also result in mixed obstructive and

restrictive physiology, or even in a purely restrictive process in some patients (1).

Prospective evaluation of pulmonary function parameters in bronchodilator trials in patients with emphysema has shown that responders exhibit an improvement in FEV₁ and a decline in FRC, RV, and TLC (13). In contrast, MILES patients in the sirolimus arm showed no differences in RV and a small increase in FRC, despite an improvement in FEV₁ (4).

The baseline to 12-month changes in VC in the placebo and sirolimus groups in our study population were similar in direction and magnitude, whether measured by spirometry (Table E5) or by CT (Table 4). For estimation of lung volume changes, however, the plethysmographic measurements of RV in the MILES cohort revealed no between-group differences, while the CT-derived baseline to 12-month increases in RV tended to be less in the sirolimus group than in the placebo group, only narrowly missing statistical significance ($P = 0.05$) (Table 4). The RV/TLC ratio was significantly different between the two groups, with the sirolimus group demonstrating a 1% decline and the placebo group having a 5% increase from baseline.

The CT-derived TLC trended toward a greater increase in the sirolimus

group than in the placebo group over the course of the treatment period.

Volumetric assessment of the lung using CT is arguably more accurate than plethysmographic lung volumes as it allows for three-dimensional analysis of the lung boundaries, enabling accurate calculation of volumes at TLC and RV (14). In addition, the measurement of RV by plethysmography in the laboratory requires mastery of adequate technique by the patient (e.g., coordination, cooperation) and is among the most variable and effort dependent of all PFTs (15).

The CT-based analysis in this study showed a worsening of air trapping in the placebo arm and stabilization in the sirolimus arm, as measured by RV and RV/TLC ratio. The mechanism of progressive gas trapping appears to be a limitation in emptying of cystic airspaces, based on stunted expiratory cyst volume transitions seen in the placebo group and preserved respiratory cycle cyst volume excursions in the sirolimus group by Markov chain analysis.

This result adds another dimension to the debate about whether the primary benefit of sirolimus on VC in LAM is an improvement in lung compliance due to reduction in LAM cell burden or an improvement in airflow obstruction and dynamic hyperinflation (16). Taken together, the CT-derived data suggest that sirolimus facilitates cyst emptying during expiration, improving FVC and attenuating progressively worsening gas trapping (RV) due to LAM (Figures 4 and 5).

Differences in RV estimates by gas dilution and plethysmography in 190 patients enrolled in the LAM Registry (103.2 ± 2.3 ml and 125.4 ± 4.6 ml, respectively) suggest that not all cysts

Table 4. Changes in computed tomography–derived lung volumes from baseline to 12 months

Variable	Placebo (n = 14)	Sirolimus (n = 17)	P Value
Change in median TLC, ml	+19.0 (−67.2, +129.7)	+25.5 (−158.8, +165.6)	0.77
Change in median VC, ml	−190.4 (−584.9, −65.6)	+15.5 (−221.4, +305.8)	0.075
Change in median RV, ml	+214.4 (+109.2, +432.6)	+2.92 (−263.9, +246.9)	0.054
Change in RV/TLC	+0.05 (0.02, 0.08)	−0.01 (−0.05, 0.05)	0.0498

Definition of abbreviations: RV = residual volume; TLC = total lung capacity. Upper and lower quartiles are given in parentheses.

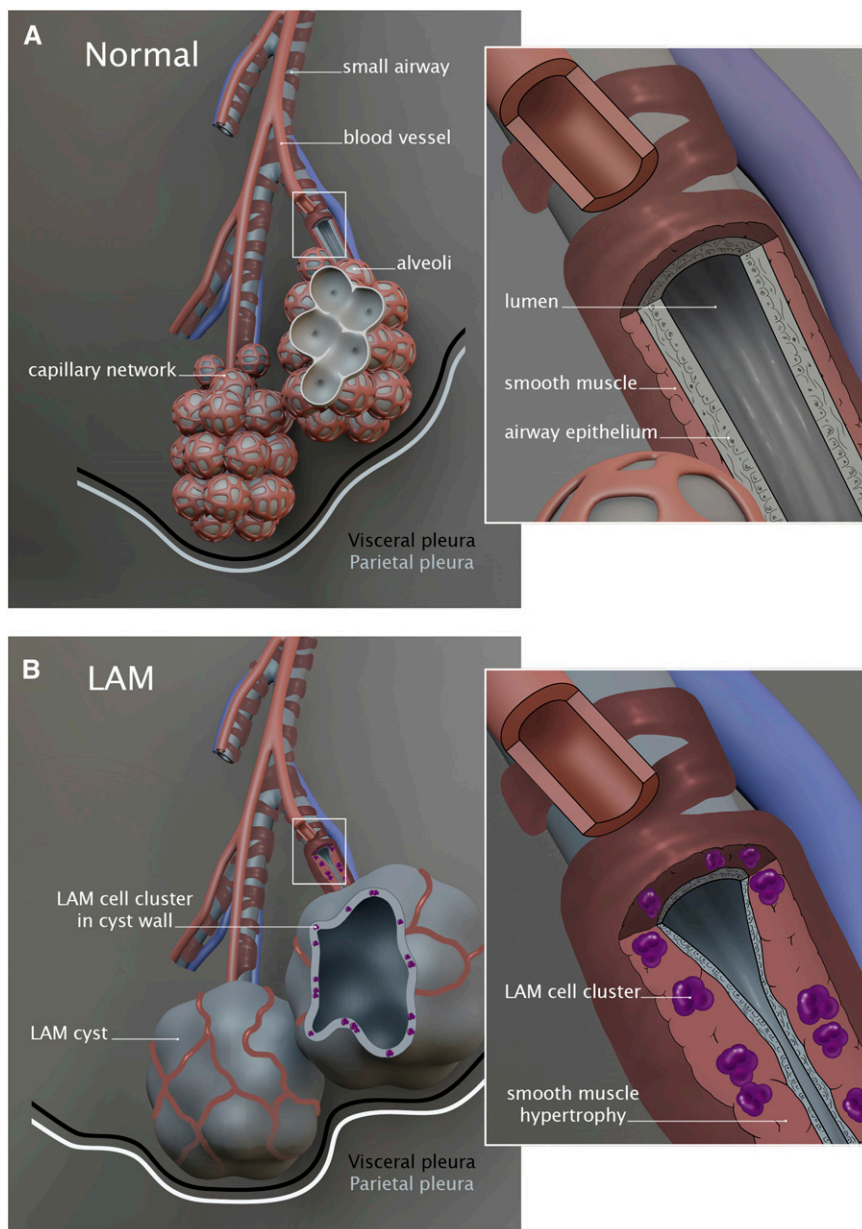


Figure 4. Graphic illustration of the mechanism of airflow obstruction in lymphangiomyomatosis (LAM). (A) Normal bronchioles and terminal airways and (B) small airways in LAM with LAM cell clusters in the airway walls with associated smooth muscle hypertrophy.

communicate with the airspaces in LAM (1). However, the characteristic speckled pattern seen on xenon ventilation scans of patients is consistent with tracer deposition in dilated distal airspaces (7). Our results derived from the Markov chain analysis, in which cysts became smaller during the respiratory cycle from inspiration to expiration, indicate that a significant fraction of cysts directly communicate with the airways.

Because sirolimus targets the mTOR pathway, inhibits cell proliferation, and reduces cell volume, a drug-induced decrease in LAM cell burden or size in the cyst walls and the small airways is a plausible explanation for the preserved respiratory cycle cyst size excursions and reduction in gas trapping in the group that was treated with the active agent.

Intrathoracic LAM manifestations beyond cystic remodeling, such as chylous

effusions, pleural thickening, and parenchymal lymphatic congestion, can affect lung function and respond to sirolimus treatment (17). For this reason, we excluded cases with these pathologies to accurately define the impact of sirolimus on cyst size characteristics and physiology. As a result, our data reflect the isolated CT effects of sirolimus on parenchymal and airway disease in LAM.

This study has several limitations. Patients were excluded if they did not have either a baseline or 12-month CT scan, had suboptimal images, or had pleural or parenchymal abnormalities, which may have introduced biases. As a result, the data derived from the smaller subset of patients in the MILES CT cohort may have limited our ability to validate physiologic trends that were apparent in the larger MILES cohort with certainty (such as a robust increase in VC). The watershed algorithm used in this study is a new quantitative CT method for estimating cyst volume and cyst numbers. Further prospective studies are needed to validate the utility of the technique in cystic lung disease. In that regard, in a recent preliminary study in which Lo and colleagues employed cyst parameters obtained via the watershed technique, a good correlation with spirometric measures of FEV₁ and FVC in patients with LAM was demonstrated (11).

In conclusion, quantitative CT analysis revealed that sirolimus improved airflow obstruction and reduced air trapping in patients with LAM. We speculate that sirolimus increases lung compliance by reducing LAM cell infiltration in the small airways, allowing relief of airflow obstruction, and/or by reducing the LAM cell burden in the lung parenchyma. Quantitative imaging modalities such as cyst volumetric analysis are promising tools to complement lung function testing and serum VEGF-D measurement in trials and in the therapeutic monitoring of patients with LAM. ■

Author disclosures are available with the text of this article at www.atsjournals.org.

Acknowledgment: The authors acknowledge the contributions of their graphics illustrator, Ms. Emma Vought (clinical instructor, neurosciences, MUSC), who was responsible for the graphic depictions of LAM pathophysiology.

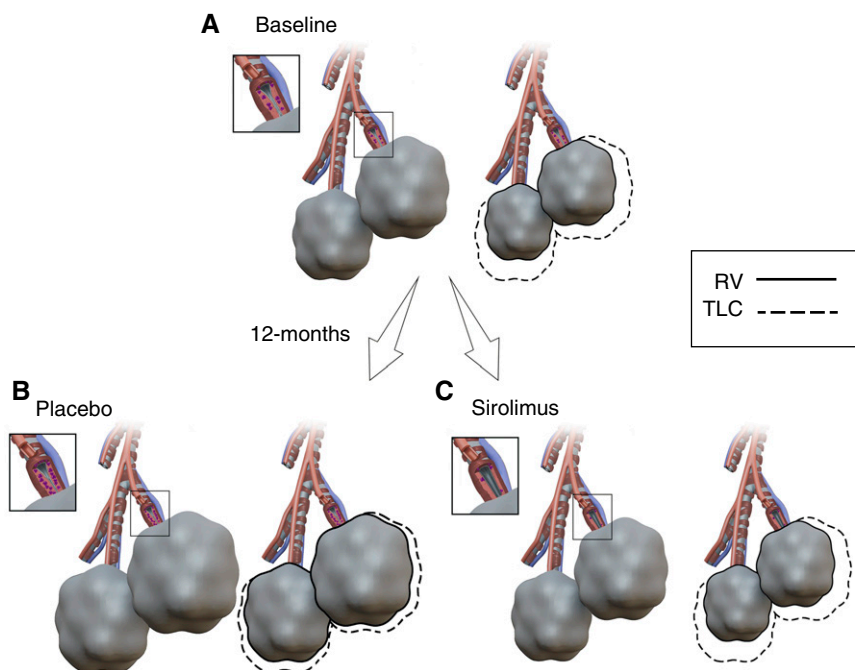


Figure 5. An illustration of the mechanism of impact of sirolimus on hyperinflation in lymphangioleiomyomatosis (LAM). (A) LAM airways and cysts at baseline. Sirolimus improves the LAM cell burden in the airways and thus improves airway obstruction and results in better cyst emptying at 12 months (C) compared with the placebo group with persistent or worsening airflow obstruction and stunted cyst transitions at 12 months (B). RV = residual volume; TLC = total lung capacity. *Inset boxes* represent the LAM cell cluster densities at baseline (A), the placebo group at 12 months (B), and the sirolimus group at 12 months (C).

References

- Ryu JH, Moss J, Beck GJ, Lee JC, Brown KK, Chapman JT, Finlay GA, Olson EJ, Ruoss SJ, Maurer JR, *et al.*; NHLBI LAM Registry Group. The NHLBI lymphangioleiomyomatosis registry: characteristics of 230 patients at enrollment. *Am J Respir Crit Care Med* 2006;173:105–111.
- Henske EP, McCormack FX. Lymphangioleiomyomatosis – a wolf in sheep's clothing. *J Clin Invest* 2012;122:3807–3816.
- Meraj R, Wikenheiser-Brokamp KA, Young LR, McCormack FX. Lymphangioleiomyomatosis: new concepts in pathogenesis, diagnosis, and treatment. *Semin Respir Crit Care Med* 2012;33:486–497.
- McCormack FX, Inoue Y, Moss J, Singer LG, Strange C, Nakata K, Barker AF, Chapman JT, Brantly ML, Stocks JM, *et al.*; National Institutes of Health Rare Lung Diseases Consortium; MILES Trial Group. Efficacy and safety of sirolimus in lymphangioleiomyomatosis. *N Engl J Med* 2011;364:1595–1606.
- Young L, Lee HS, Inoue Y, Moss J, Singer LG, Strange C, Nakata K, Barker AF, Chapman JT, Brantly ML, *et al.*; MILES Trial Group. Serum VEGF-D a concentration as a biomarker of lymphangioleiomyomatosis severity and treatment response: a prospective analysis of the Multicenter International Lymphangioleiomyomatosis Efficacy of Sirolimus (MILES) trial. *Lancet Respir Med* 2013;1:445–452.
- Corrin B, Liebow AA, Friedman PJ. Pulmonary lymphangioleiomyomatosis: a review. *Am J Pathol* 1975;79:348–382.
- Chu SC, Horiba K, Usuki J, Avila NA, Chen CC, Travis WD, Ferrans VJ, Moss J. Comprehensive evaluation of 35 patients with lymphangioleiomyomatosis. *Chest* 1999;115:1041–1052.
- Baldi BG, Albuquerque AL, Pimenta SP, Salge JM, Kairalla RA, Carvalho CR. Exercise performance and dynamic hyperinflation in lymphangioleiomyomatosis. *Am J Respir Crit Care Med* 2012;186:341–348.
- Chilosi M, Pea M, Martignoni G, Brunelli M, Gobbo S, Poletti V, Bonetti F. Cathepsin-K expression in pulmonary lymphangioleiomyomatosis. *Mod Pathol* 2009;22:161–166.
- Avila NA, Kelly JA, Dwyer AJ, Johnson DL, Jones EC, Moss J. Lymphangioleiomyomatosis: correlation of qualitative and quantitative thin-section CT with pulmonary function tests and assessment of dependence on pleurodesis. *Radiology* 2002;223:189–197.
- Lo P, Brown MS, Kim H, Kim H, Argula R, Strange C, Goldin JG. Cyst-based measurements for assessing lymphangioleiomyomatosis in computed tomography. *Med Phys* 2015;42:2287–2295.
- Bissler JJ, McCormack FX, Young LR, Elwing JM, Chuck G, Leonard JM, Schmithorst VJ, Laor T, Brody AS, Bean J, *et al.* Sirolimus for angiomyolipoma in tuberous sclerosis complex or lymphangioleiomyomatosis. *N Engl J Med* 2008;358:140–151.
- O'Donnell DE, Flüge T, Gerken F, Hamilton A, Webb K, Aguilaniu B, Make B, Magnussen H. Effects of tiotropium on lung hyperinflation, dyspnoea and exercise tolerance in COPD. *Eur Respir J* 2004;23:832–840.
- Brown MS, Kim HJ, Abtin F, Da Costa I, Pais R, Ahmad S, Angel E, Ni C, Kleerup EC, Gjertson DW, *et al.* Reproducibility of lung and lobar volume measurements using computed tomography. *Acad Radiol* 2010;17:316–322.
- Teculescu DB, Bohadana AB, Peslin R, Pino J, Jansen da Silva JM. Variability, reproducibility and observer difference of body plethysmographic measurements. *Clin Physiol* 1982;2:127–138.
- Burger CD. Efficacy and safety of sirolimus in lymphangioleiomyomatosis. *N Engl J Med* 2011;365:271–272.
- Taveira-DaSilva AM, Hathaway O, Stylianou M, Moss J. Changes in lung function and chyloous effusions in patients with lymphangioleiomyomatosis treated with sirolimus. *Ann Intern Med* 2011;154:797–805, W-292–W-293.